Science of the Total Environment 639 (2018) 624–632

Contents lists available at ScienceDirect

Science of the Total Environment

journal homepage: www.elsevier.com/locate/scitotenv

Surface accumulation of low molecular weight dissolved organic matter in surface waters and horizontal off-shelf spreading of nutrients and humic-like fluorescence in the Chukchi Sea of the Arctic Ocean

Meilian Chen [a,b], Jinyoung Jung [c], Yun Kyung Lee [a], Jin Hur [a,*]

[a] Department of Environment & Energy, Sejong University, Seoul 05006, South Korea
[b] Environmental Program, Guangdong Technion - Israel Institute of Technology, Shantou 515063, China
[c] Division of Polar Ocean Science, Korea Polar Research Institute, Incheon 21990, South Korea

HIGHLIGHTS

- Spatial distribution of DOM was examined in a highly productive polar sea.
- Low molecular weight (M_n < ~350 Da) DOM molecules tend to be accumulated in surface ocean.
- Horizontal off-shelf spreading of nutrients and humic-like fluorescence was found.
- The study suggests sea ice treat in the Arctic Ocean can potentially accelerate primary productivity and DOC increase.
- It provides a new insight into DOM dynamics and the roles in future polar oceans.

GRAPHICAL ABSTRACT

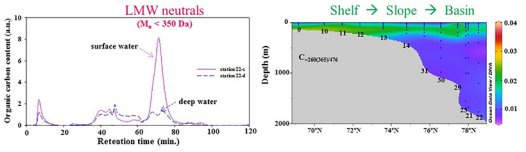

ARTICLE INFO

Article history:
Received 16 April 2018
Received in revised form 17 May 2018
Accepted 17 May 2018
Available online 26 May 2018

Editor: D. Barcelo

Keywords:
Arctic Ocean
EEM-PARAFAC
SEC-OCD
Productivity
FT-ICR-MS

ABSTRACT

Polar regions play unique roles in global overturning circulation, carbon cycling, and climate change. In this study, seawater dissolved organic matter (DOM) was characterized for the Chukchi Sea in the Arctic Ocean in the summer season. The seawater generally contains high concentrations of dissolved organic carbon (DOC, up to 92 μM C) and tyrosine-like fluorescence (up to 0.21 RU), and it was enriched with heteroatomic molecular formula with nitrogen-containing and sulfur-containing formulas counting 2246 (~41% of total identified molecular formula) and 1838 (~34%), respectively. Significant correlations were observed between salinity and the absorption coefficient at 254 nm, between chlorophyll-*a* and DOC as well as the tyrosine-like component, $C_{270/302}$ ($C_{ex/em}$ maxima), and between biological index and two protein-like components, $C_{275/338}$ and $C_{305/344}$. A comparison between surface waters and close-to-seafloor deep waters suggested a trend of the accumulation of low molecular weight (LMW) fraction (~54–74%, nominal average molecular weight M_n < ~350 Da) in the surface waters. Another interesting finding from spatial data was an obvious horizontal off-shelf spreading of nutrients and humic-like fluorescence. This study sheds novel insights of DOM characteristics and dynamics in the highly productive polar sea.

© 2018 Elsevier B.V. All rights reserved.

1. Introduction

The Arctic Ocean, being super sensitive to the ongoing climate change, plays pivotal roles in global biogeochemical cycles. Approximately

* Corresponding author.
E-mail address: jinhur@sejong.ac.kr (J. Hur).

https://doi.org/10.1016/j.scitotenv.2018.05.205
0048-9697/© 2018 Elsevier B.V. All rights reserved.

1100–1500 Pg of organic carbon is stored in the Arctic soils (Rachold et al., 2004). Moreover, the Arctic Ocean sinks ~5–14% of the total anthropogenic CO_2 emission (Bates et al., 2011).

DOM in the Arctic Ocean is known to originate from riverine runoff, coastal erosion, aeolian input, benthic efflux from sediments, sea ice, and autochthonous primary productivity (Stein, 2008; Chen et al., 2016a). In addition, microbes have been reported to play a powerful role in glacial environments (including supra-, en-, and sub-glacial) in the Arctic (Musilova et al., 2017). The biological index (BIX) was found to be positively correlated with temperature as well as protein-like fluorescence in a previous study in the Chukchi Sea of the Arctic (Chen et al., 2017a). With the ongoing sea ice retreating and thinning, recent studies conducted in the Arctic Ocean provided evidence on widespread shift to double algal blooms (both spring and fall, Ardyna et al., 2014; Uchimiya et al., 2016; Chen et al., 2017a) and the ice algae derived DOM contributed by ice-edge upwelling phytoplankton bloom (mostly, *Phaeocystis pouchetii*) (Mundy et al., 2009; Assmy et al., 2017). A fall phytoplankton bloom leading to high protein-like fluorescence is also noteworthy in recent studies on the Chukchi Sea of the Arctic Ocean (Chen et al., 2017a). Furthermore, it was previously reported that humic-like DOM and nutrients could be spread laterally in cold dense subsurface water of the Arctic Ocean (Hioki et al., 2014).

Despite the several DOM studies conducted in the Arctic Ocean (Walker et al., 2009; Guéguen et al., 2012, 2014, 2015; Tanaka et al., 2016; Chen et al., 2017a), they primarily used optical methods or studied the surface waters only, which could limit the full understanding of DOM in the Arctic Ocean. Thus, we investigated here the dynamics of DOM through the entire water column, and also utilized three analytical tools for DOM characterization, including fluorescence excitation emission matrix coupled with parallel factor analysis (EEM-PARAFAC), high-resolution Fourier transform ion cyclotron resonance mass spectrometry (FT-ICR-MS), and size exclusion chromatography with an organic carbon detector (SEC-OCD), which allowed to probe DOM fluorescent and molecular signatures and molecular weight distribution. The Chukchi Sea was chosen as a highly productive sea, which has a DOC production rate of ~35 mmol C m^{-2} d^{-1} (Yun et al., 2016). This Sea is known to be an important source of organic matter in the Western Arctic due to its high primary productivity driven by the nutrient-enriched Bering Shelf Anadyr Water (BSAW) entraining through the Bering Strait (Sakshaug, 2004).

2. Materials and methods

2.1. Site description and water mass properties

Sampling sites are located in the Chukchi Sea of the Arctic Ocean (Fig.1). The Chukchi Sea is well known for seasonal sea ice cover and high primary productivity. In the Arctic Ocean, water masses usually include a low-salinity Arctic Surface Water (ASW: <50 m), a complex Halocline Intermediate Water (HIW: 50–200 m, Pacific-derived on the Bering Strait side while Atlantic-derived on the Fram Strait side), a warm and saline Atlantic Deep Water (ADW), and a layer of Arctic Bottom Water (ABW > 900 m, Fig. 2).

2.2. Field sampling

Hydrographic surveys and seawater sampling were carried out at 12 stations in the Chukchi Sea, using a conductivity-temperature-depth (CTD) and a rosette system holding 24 10 L-Niskin bottles (SeaBird Electronics, SBE 911 plus) aboard the Korean icebreaker R/V *Araon* during the ARA07B (August 6th to 19th, 2016) cruise. The twelve sites in the Chukchi Sea spanned along a shelf to slope and basin gradient with four ice-free sites (Fig.1, red labels) and the remainders were partially ice-covered (blue labels) at the sampling time.

Samples for DOC analysis were drawn from the Niskin bottle by gravity filtration through an inline pre-combusted (at 550 °C for 6 h) Whatman GF/F borosilicate glass fiber filter held in an acid-cleaned (0.1 M HCl) polycarbonate 47 mm filter holder (PP-47, ADVANTEC). The filter holder was attached directly to the Niskin bottle spigot. The filtrate (~250 ml) was collected in an acid-cleaned glass bottle after ~100 ml of seawater was passed through to clean the sampling system. The collected samples were distributed into two pre-combusted 20 ml glass ampoules with a sterilized serological pipette. Each ampoule was sealed with a torch, quick-frozen, and preserved at −24 °C until further analyses in land laboratory within about two months. Samples for inorganic nutrient analyses were pre-filtered in a manner similar to that for DOC, transferred to a 50 ml conical tube and immediately stored in a refrigerator at 2 °C prior to chemical analysis onboard within 3 days.

2.3. Onboard analyses

The nutrients were measured onboard after sampling using a four-channel continuous Auto-Analyzer (QuAAtro, Seal Analytical) according

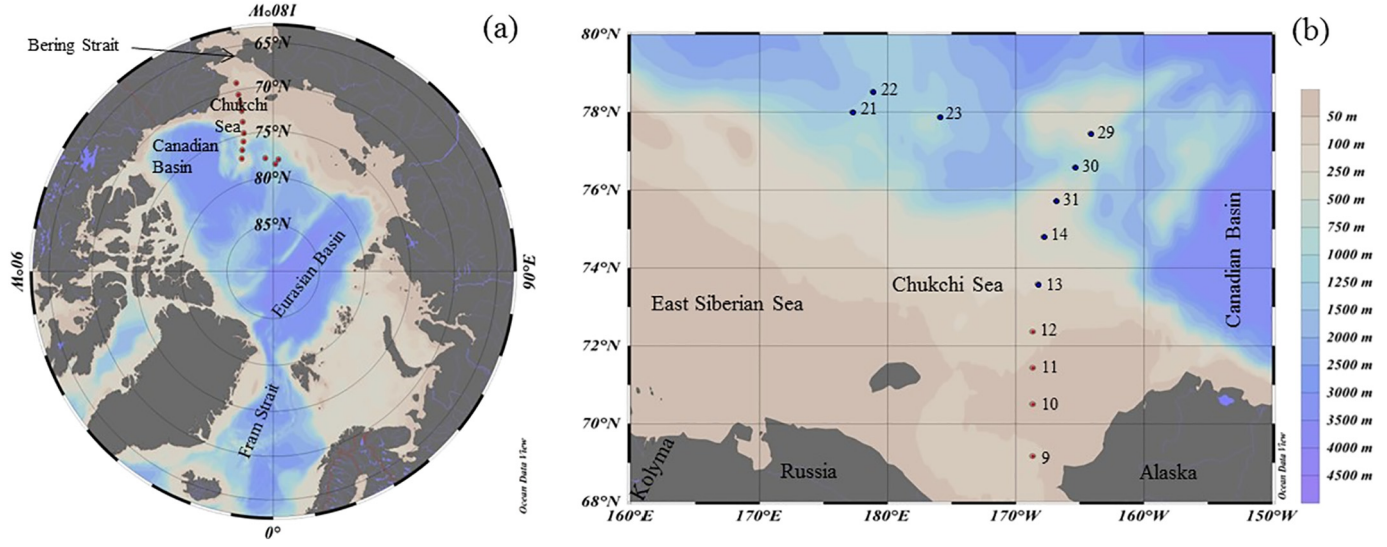

Fig. 1. Sampling sites in the Chukchi Sea, Arctic. Ice-free and ice-covered sites are marked with red and blue colors, respectively. The sea ice concentration data from Aug. 6th to Aug. 19th in the Arctic are obtained from http://www.meereisportal.de. The maps were created with Ocean Data View (Schlitzer, 2017).

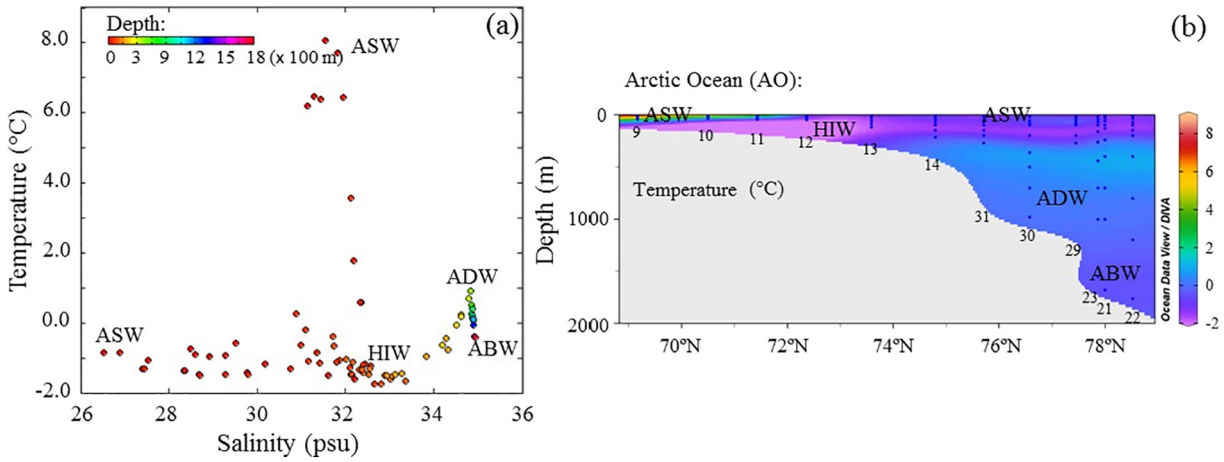

Fig. 2. Property-property plot of θ-S and section plot temperature of all seawater samples. Water mass types identified include: Arctic Surface Water (ASW: <50 m), Halocline Intermediate Water (HIW, 50–200 m), Atlantic Deep Water (ADW), and Arctic Bottom Water (ABW, >900 m) in the Chukchi Sea, the Arctic Ocean.

to the Joint Global Ocean Flux Study (JGOFS) protocols described elsewhere (Gordon et al., 1993). The precision for NH_4^+, $NO_3^- + NO_2^-$, PO_4^{3-}, and $Si(OH)_4$ measurements were ±0.18, ±0.14, ±0.02, and ±0.28 μmol L^{-1}, respectively. Seawater samples for chlorophyll *a* (chl-*a*) measurement were collected in the upper 100 m and filtered onto 47 mm GF/F filters under low vacuum pressure. Filters were extracted with 90% acetone for 24 h (Parsons et al., 1984), and then measured onboard using a fluorometer at excitation/emission wavelengths of 470/695 nm (Trilogy, Turner Designs, USA).

2.4. DOC analyses

DOC was measured using a Shimadzu TOC-L analyzer based on high temperature combustion. Milli-Q water (blank) and consensus reference material (CRM, 42–45 μM C for DOC, deep Florida Strait water obtained from University of Miami, Miami, Florida, U.S.A.) were measured every sixth analysis to check the accuracy of the measurements. Analytical errors based on replicated measurements (at least three measurements per sample) were within 5% for DOC.

2.5. UV–vis and EEM measurements

Absorption spectra were obtained from 240 to 800 nm on a Shimadzu 1800 ultraviolet-visible (UV–Vis) spectrophotometer (Shimadzu Inc., Japan). 3D fluorescence EEMs were scanned using a Hitachi F-7000 luminescence spectrometer (Hitachi Inc., Japan) at the excitation/emission (Ex/Em) wavelengths of 250–500/280–550 nm as in a prior report (Chen et al., 2016a). The excitation and the emission scans were set at 5 nm and 1 nm steps, respectively. The procedures of post-acquisition corrections are carried out as described previously (Chen et al., 2010). Briefly, inner filer effect was corrected using UV–Vis data according to literature (McKnight et al., 2001). Instrumental biases were corrected automatically by the installed settings. Blank subtraction was performed using Milli-Q water. The area under the Milli-Q water Raman peak at excitation 350 nm was used for the correction to daily fluorescence variation based on the literature (Cory and McKnight, 2005). All fluorescence measurements were converted to Raman Unit (RU) according to a previous literature (Lawaetz and Stedmon, 2009). PARAFAC modeling was performed using the MATLAB7.0.4 with the DOMFluor toolbox (Stedmon and Bro, 2008). All corrected EEMs of seawater in the Arctic Ocean ($n = 89$) were used for modeling. The number of fluorescent components was determined based on the split-half validation. Biological index (BIX), an index of recent biological and autochthonous contribution, was calculated according to literature (BIX = F_{380}/F_{430} at excitation 310 nm, where F represents emission fluorescence intensity, Huguet et al., 2009).

2.6. SEC-OCD measurements

SEC (chromatographic column: 250 × 20 mm, TSK, HW 50S; Toso, Japan) coupled with an OCD (DOC Labor Dr. Huber, Karlsruhe, Germany) was performed to measure the molecular weight (MW) distribution for representative samples for surface seawaters (≤30 m) and close-to-seafloor deep seawaters (~1700 m at station 22 and ~980 m at station 30). A mobile phase containing a phosphate buffer of pH 6.85 was used with a flow rate of 1.1 mL min^{-1}. Detailed configuration and method description of this system are available elsewhere (Huber et al., 2011; Chen et al., 2016b).

2.7. FT-ICR-MS measurements

FT-ICR-MS measurements were carried out with a 15-T FT-ICR-MS interfaced with an Apollo II electrospray ionization source (ESI, Bruker Daltonik, Germany) in negative ion mode. Due to limited sample volume of each sample and the large volume needed for pre-treatment, we combined the samples from all the stations and depths from Arctic Ocean for FT-ICR-MS measurement. The solid phase extraction (SPE) using BondElut cartridges (1 g PPL sorbent, Agilent Inc.) was performed prior to the FT-ICR-MS measurements as described elsewhere (Dittmar et al., 2008). One liter of the acidified sample (with high-performance liquid chromatography grade HCl) was discharged through the PPL cartridge. After all the samples passed though the cartridge, the PPL cartridge was dried up completely with high purity N_2, and then the adsorbed DOM on the cartridge was eluted immediately with 6 ml of methanol into a glass ampoule. The samples were stored in −20 °C immediately and were measured in one week. Sample was injected with a Hamilton syringe with a flow rate of 2 μl min^{-1}. Negatively charged ions were accumulated in an argon-filled collision cell for 1 s and transferred to the ICR cell. A S/N ratio of ≥4 was set. The spectra were evaluated in the mass range of *m/z* 200–650. The following elemental ratio criteria were implemented: 2.2 > H/C > 0.3, O/C < 1.2. The double bond equivalent (DBE) was calculated based on the formula: DBE = 1 + 1/2(2C − H + N) (Koch and Dittmar, 2006). A detailed method description is available in previous reports (Chen et al., 2016c, 2016d).

3. Results

3.1. Depth profile and spatial variations of DOM in ice-free vs. ice-covered sites

The depths of the sampled water spanned from 3 to 1762 m in the Chukchi Sea. The DOC and a_{254} values generally accumulated in the surface layer with the maximum values reaching up to ~92 μM and

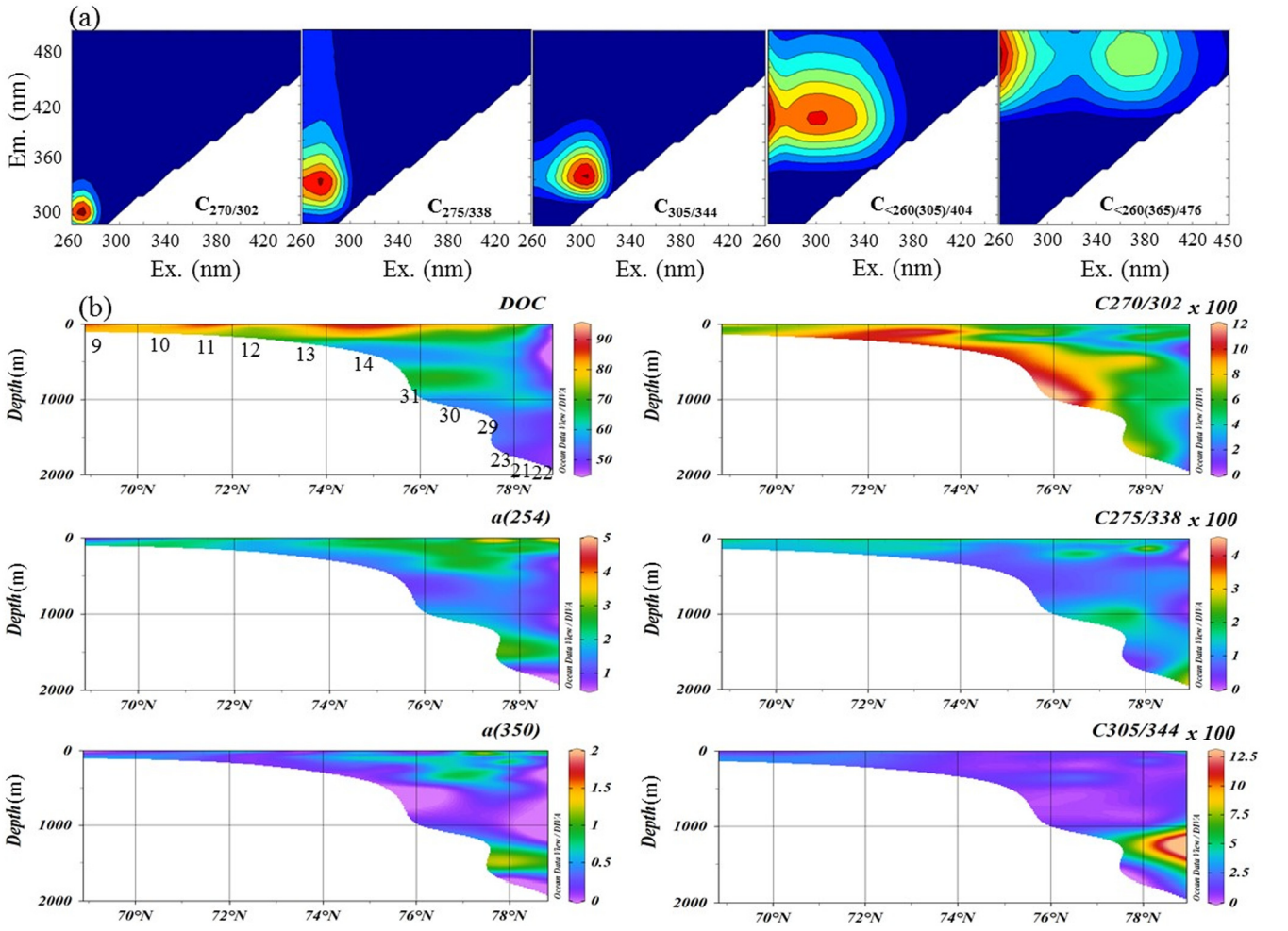

Fig. 3. Contour plots of identified five EEM-PARAFAC components (a) and section plots of DOM parameters (b) for seawaters. The excitation/emission maxima of components (Ex/Em) are listed as shown in (a).

~5.0 m^{-1}, respectively (Fig. 3). Based on the section plots in Fig. 3, the tyrosine-like $C_{270/302}$ (i.e., a EEM-PARAFAC component with the peak at the Ex/Em of 270/302 nm) potentially have a sediment-derived source from the continental shelf and slope with very high levels at the bottom, which was supported by the production of tyrosine-like DOM and its benthic efflux from marine sediments previously reported in the Chukchi Sea (Chen et al., 2016a).

The sampling stations were categorized into ice-free and ice-covered (> 15% coverage) sites to facilitate the comparison among the sites and to assess the potential effects of ongoing sea ice retreat. The DOC concentration reached up to 83 ± 5 μM and 70 ± 11 μM for ice-free and ice-covered sites, respectively (Table 1). These values are generally comparable to those in prior reports of the Arctic Ocean (Table S1). The current consensus is that DOC is enriched by the terrigenous inputs via fluvial input in the highly stratified Arctic Ocean (Dittmar and Kattner, 2003). Moreover, the ice-free sites featured higher DOC concentrations than the ice-covered sites ($p < 0.01$), implying potential higher primary productivity at ice-free sites due to higher light availability.

The absorption coefficients of chromophoric DOM (CDOM) at 254 nm and 350 nm (namely, a_{254} and a_{350}, $a_\lambda = 2.303 \times A_\lambda$/pathlength, where A_λ is the optical density, Blough and Del Vecchio, 2002) were 1.9 ± 0.6 m^{-1} at ice-free sites and 2.2 ± 0.8 m^{-1} at ice-covered sites for a_{254} and 0.3 ± 0.3 m^{-1} at ice-free sites and 0.4 ± 0.4 m^{-1} at ice-covered sites for a_{350}. The observed CDOM absorption coefficient levels were generally comparable to those in previous reports (Table S1). However, no significant differences were found in the two absorption coefficients between ice-free and ice-covered sites.

For fluorescent DOM (FDOM), five EEM-PARAFAC components were identified (Fig. 3). The component of $C_{270/302}$ was assigned as tyrosine-like component, while $C_{275/338}$ spectra was similar to tryptophan-like component. The $C_{305/344}$ resembled the sea ice-related protein-like component previously reported (Stedmon et al., 2011). In addition to

Table 1
Summary of bulk DOC, absorption coefficient of CDOM, and fluorescence data.

DOM items	Assignment	Unit	Ice-free sites	Ice-covered sites
Chl-*a*	–	mg m^{-3}	0.8 ± 0.7	0.2 ± 0.3
DOC	–	μM	83 ± 5	70 ± 11
CDOM:				
a_{254}	–	m^{-1}	1.9 ± 0.6	2.2 ± 0.8
a_{350}	–	m^{-1}	0.3 ± 0.3	0.4 ± 0.4
FDOM:				
$C_{270/302}$	Tyrosine-like	RU	0.07 ± 0.01	0.06 ± 0.03
$C_{275/338}$	Tryptophan-like	RU	0.02 ± 0.01	0.01 ± 0.01
$C_{305/344}$	Protein-like	RU	0.02 ± 0.01	0.02 ± 0.05
$C_{<260(305)/404}$	Humic-like	RU	0.02 ± 0.00	0.02 ± 0.01
$C_{<260(365)/476}$	Terrestrial humic-like	RU	0.01 ± 0.00	0.01 ± 0.01
$C_{270/302}$	–	%	50 ± 8	46 ± 14
$C_{275/338}$	–	%	12 ± 4	11 ± 5
$C_{305/344}$	–	%	13 ± 6	12 ± 12
$C_{<260(305)/404}$	–	%	15 ± 2	18 ± 5
$C_{<260(365)/476}$	–	%	10 ± 2	13 ± 5

the three protein-like components, one traditionally termed marine humic-like component, $C_{<260(305)/404}$, and one red-shifted terrestrial humic-like component, $C_{<260(365)/476}$, were found. These results were consistent with the prior findings of humic-like FDOM in the Chukchi Sea although the excitation/emission maxima are not identical (Guéguen et al., 2012; Chen et al., 2017a; Mendoza et al., 2017).

The tyrosine-like fluorescence $C_{270/302}$ averaged 0.06 ± 0.03 RU and 0.07 ± 0.01 RU for ice-covered and ice-free sites, respectively (Table 1). For the tryptophan-like component $C_{275/338}$, it averaged 0.01 ± 0.01 RU and 0.02 ± 0.01 RU for ice-covered and ice-free sites, respectively. The tyrosine-like fluorescence levels were higher than those reported previously in the same region (0.03 RU, Logvinova et al., 2015) but were lower than those observed during a month-long fall phytoplankton (0.24 RU, Chen et al., 2017a). The chl-*a* data of ~0.8 mg m^{-3} was higher than the threshold of 0.5 mg m^{-3} generally indicative of algal bloom in this region (Perrette et al., 2011; Ardyna et al., 2014), suggesting the occurrence of algal blooms at the ice-free sites which might contribute to the relatively higher tyrosine-like fluorescence. In contrast, the potentially sea ice-related protein-like component $C_{305/344}$ exhibited 0.02 RU. For the humic-like component, $C_{<260(305)/404}$ and $C_{<260(365)/476}$ averaged 0.02 RU and 0.01 RU, respectively. In addition, the ice-free sites presented higher tyrosine-like $C_{270/302}$ and tryptophan-like $C_{275/338}$ than those of ice-covered sites ($p < 0.001$).

3.2. Correlations among salinity, chl-a, and DOM parameters and genesis of DOM

The salinity was found to be positively correlated with a_{254} ($r = 0.44$, $p < 0.0001$, $n = 89$, Fig. 4a), suggesting effects of terrestrial fluvial runoffs and/or sea ice melting. Both the bulk DOC and tyrosine-like $C_{270/302}$ exhibited weak but significant positive correlations with chl-*a* ($r = 0.35$ and 0.20, $n = 89$, $p < 0.001$ and 0.05, respectively, Fig. 4b), implying in situ production of the DOC and tyrosine-like fluorescence via primary productivity. In addition, tyrosine-like $C_{270/302}$ could also be derived partly from sediment inputs, particularly in the continental shelf and slope region as the higher concentrations were observed at the sites closer to the seafloor (Fig. 3). The occurrence of sediment-derived FDOM, with its origin from the production within the sediments via anaerobic respiration (e.g., sulfate reduction of particulate organic matter), is a widespread phenomenon (Burdige and Komada, 2015; Chen et al., 2016a; Chen et al., 2017b). The tryptophan-like fluorescence $C_{275/338}$ and the protein-like $C_{305/344}$ were correlated with biological index (BIX, $r = 0.95$ and 0.23, $n = 89$, $p < 0.0001$ and 0.05, respectively, Fig. 4c), suggesting the association of the two fluorescent components with microbial sources and/or the reworking. The protein-like component with an excitation wavelength around 300 nm was similar to those previously observed in the Antarctic Sea ice brine but not in seawaters (Stedmon et al., 2011), implying potential sea ice-derived origin in polar ecosystems.

Terrestrial humic-like components are typically expected in the Arctic Ocean since it receives ~10% of global river discharge while it only occupies <1% of the global ocean volume (Stein, 2008). Marine phytoplankton may also produce marine humic-like fluorescence (Romera-Castillo et al., 2010), which supports the observed levels of $C_{<260(305)/404}$ (~0.02 RU) and $C_{<260(365)/476}$ (~0.01 RU).

4. Discussion

4.1. Accumulation of LMW DOC in surface ocean

The SEC-OCD results for representative surface water samples (≤30 m) showed spiked peaks and the dominance of LMW neutrals fraction for the DOM samples (54–74%, Fig. 5; Table S2). According to the literature, this fraction has a nominal average molecular weight M_n < ~350 Da (Huber et al., 2011; Chen et al., 2016b). In sharp contrast to the surface waters, the close-to-seafloor deep waters, however,

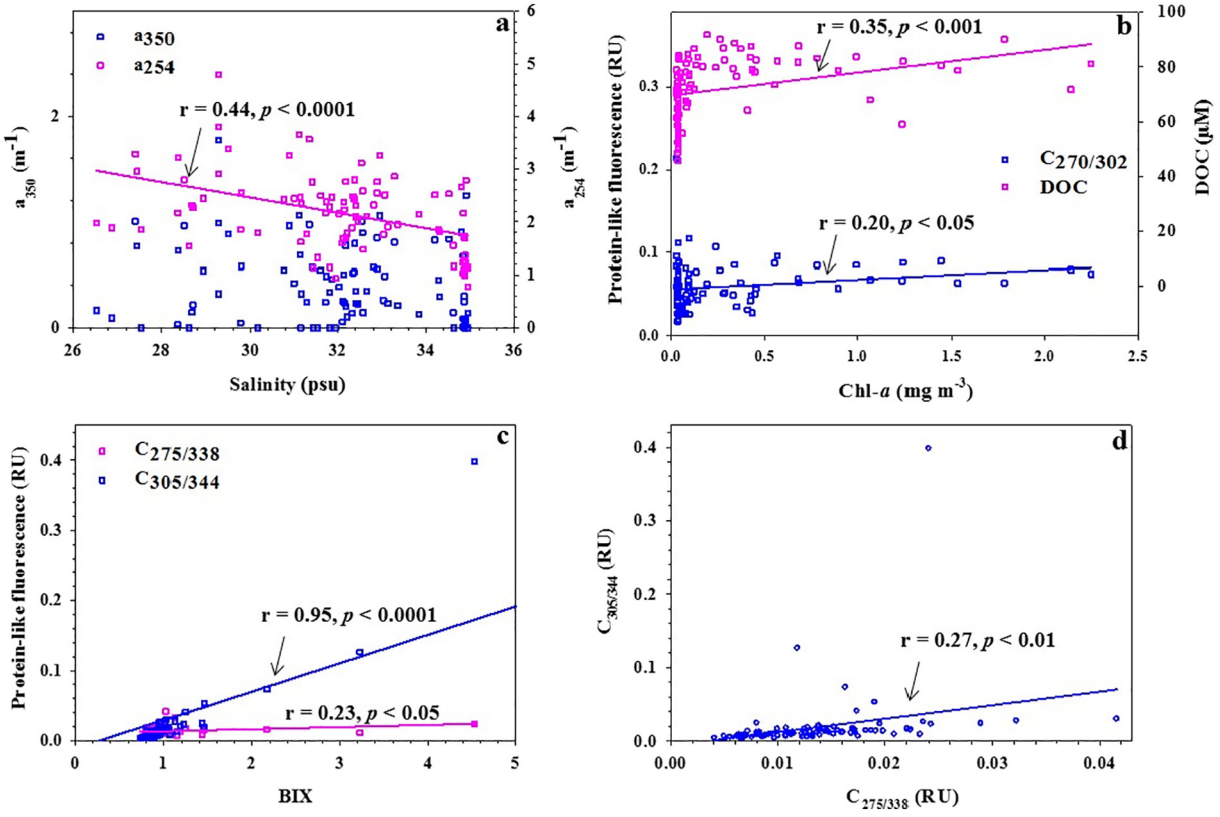

Fig. 4. Correlations between (a) salinity vs. $a_{254 \text{ and } 350}$, (b) chl-*a* vs. DOC and tyrosine-like component, (c) BIX vs. two protein-like components, and (d) two protein-like components. $n = 89$.

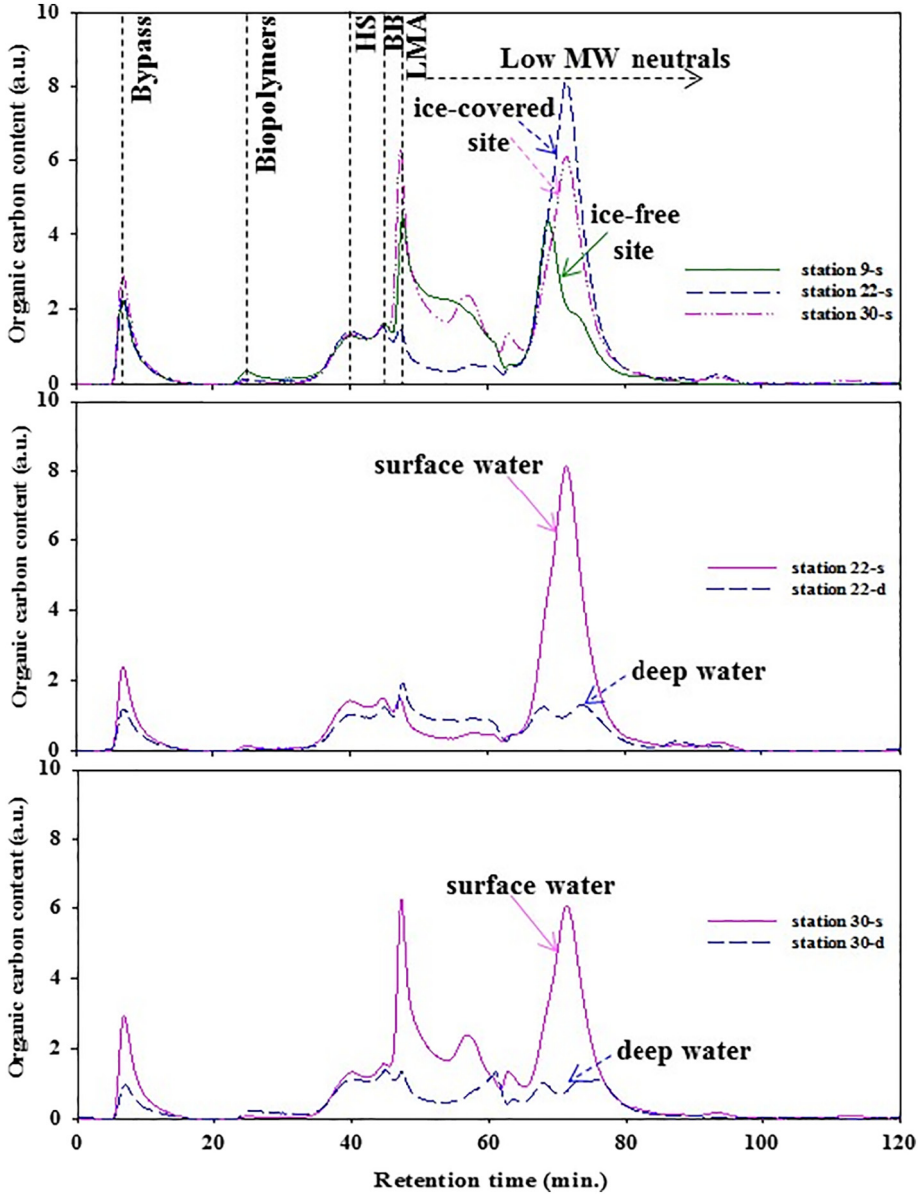

Fig. 5. SEC-OCD of representative stations. Biopolymers (M_n > 10 kDa); HS = humic substances (M_n = ~1 kDa); BB = building blocks (M_n = 350–500 Da); LMA = low molecular weight acids (M_n < 350 Da); LMW neutrals (M_n < 350 Da). M_n = nominal average molecular weight ($M_n = \Sigma N_i M_i / \Sigma N_i$, where M is the molecular mass and N is the number of molecules). Bypass was to obtain a detector signal at the dead volume time of each run. s = surface seawater (≤30 m), d = deep water (close-to-seafloor, ~1700 m at station 22 and ~980 m at station 30).

illustrated rather flat LMW fractions. The ice-covered sites 22 and 30 displayed higher amount of LMW neutrals fraction (74% and 63%, respectively) than the ice-free site 9 (54%). Ice-free site 9 had relatively more presence of humic substances fraction (18%, M_n = ~1 kDa) while site 30 spiked at building blocks fraction (26%, M_n = 350–500 Da) in the SEC chromatograms for surface waters. The building blocks fraction represents the breakdown products of humic substances which is present in most natural waters (Huber et al., 2011). The deep close-to-seafloor waters displayed relatively higher humic substances fractions than surface waters. Site 30 also spiked at the building blocks fraction and potentially affected by terrigenous DOM inputs. This site is closer to the Canadian Basin, which receives the discharge from the Mackenzie River, and the Beaufort Gyre can potentially broaden the effect to its proximity.

The results mentioned above are supported by a recent study reporting the early phytoplankton blooms dominated by *Phaeocystis pouchetii* below snow-covered sea ice in the Arctic Ocean (Assmy et al., 2017). The phenomenon of under-ice and widespread (77–89%) ice-edge phytoplankton blooms triggered by ice-edge upwelling is well-documented in the literature (Mundy et al., 2009; Perrette et al., 2011). These blooms can cause a higher ice algae primary productivity at ocean surface for ice-covered sites rather than for the ice-free site, which potentially contributed to the LMW neutrals fraction despite relatively higher bulk DOC at ice-free site 9 where more light is available (Table S2). The ice-free area can be dominated by Arctic diatoms, which probably contribute more to relatively large MW fractions of the DOC. Furthermore, the molecular formula indicated wide-spanned and heteroatom-enriched characteristics with N-containing and S-containing formula ~41% and 34%, respectively (Fig. 6 and Table S3). The total identified formula reached up to >5000 and fell into the categories of lipids-type, proteins, lignin-like/carboxyl-rich alicyclic molecules (CRAM), tannin-like, condensed aromatic compounds, indicative of a diverse of molecular compound types in the Arctic Ocean seawaters. Similar chemo-diversity was observed previously in sediment pore waters in the Amundsen and Nansen Basins of Arctic Ocean (Rossel et al., 2016).

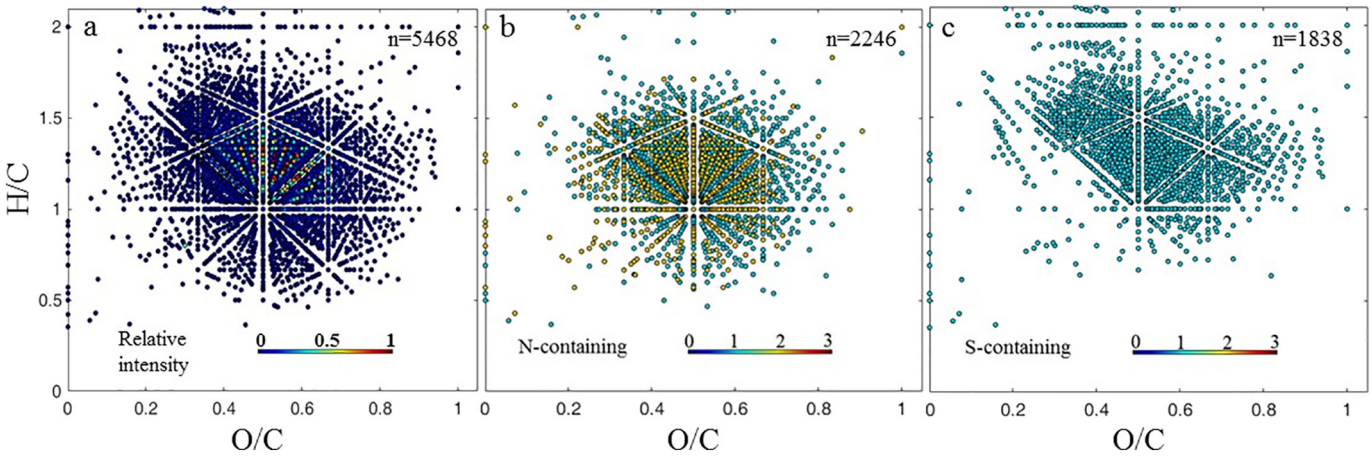

Fig. 6. Van Krevelen diagrams of the total (a), N-containing (b, 41%), and S-containing (c, 34%) formula distribution.

4.2. Horizontal off-shelf spreading of humic-like fluorescence and nutrients

It is interesting to observe an obvious off-shelf horizontal spreading (at a depth of ~100 to 200 m) of nutrients ($NO_2^- + NO_3^-$, PO_4^{3-}, and Si $(OH)_4$) and humic-like FDOM ($C_{<260(305)/404}$ and $C_{<260(365)/476}$) in the Chukchi Sea (Fig. 7), which is supported by the inferences made in previous studies (Hioki et al., 2014; Chen et al., 2017a). This phenomenon in the Arctic Ocean may be caused by the Transpolar Drift, which dominates in the Euroasian Basin. The current flow can transport nutrients and relatively refractory humic-like DOM from the shallow shelf, off the slope and further to the deeper basins. The depth of this off-shelf spreading was ~100–200 m, falling into the Halocline Intermediate Water layer. The horizontal spreading can replenish nutrients and humic-like DOM to the Arctic basins and further impacts the Arctic ecosystem. With ice retreating and permafrost thawing, more nutrients and humic-like DOM could be transported from the Arctic Shelf into the Basin. Further study is warranted to examine whether this type of off-shelf spreading exists only in the studied Chukchi Sea or it also exits in other regions of the Arctic Ocean.

5. Conclusions

Our results suggest dominance and accumulation of LMW DOC in the surface Arctic Ocean and lateral off-shelf spreading of humic-like and nutrients in the Halocline Intermediate Water layer of the Chukchi Sea. Ice-covered sites showed higher peaks for the LMW fractions than the ice-free site, presumably due to the different contributions from ice algae and Arctic diatoms. As such, the retreating sea ice in the Arctic Ocean may shift the dominant phytoplankton community as well as the DOM concentration and composition. Furthermore, the higher chl-*a* and

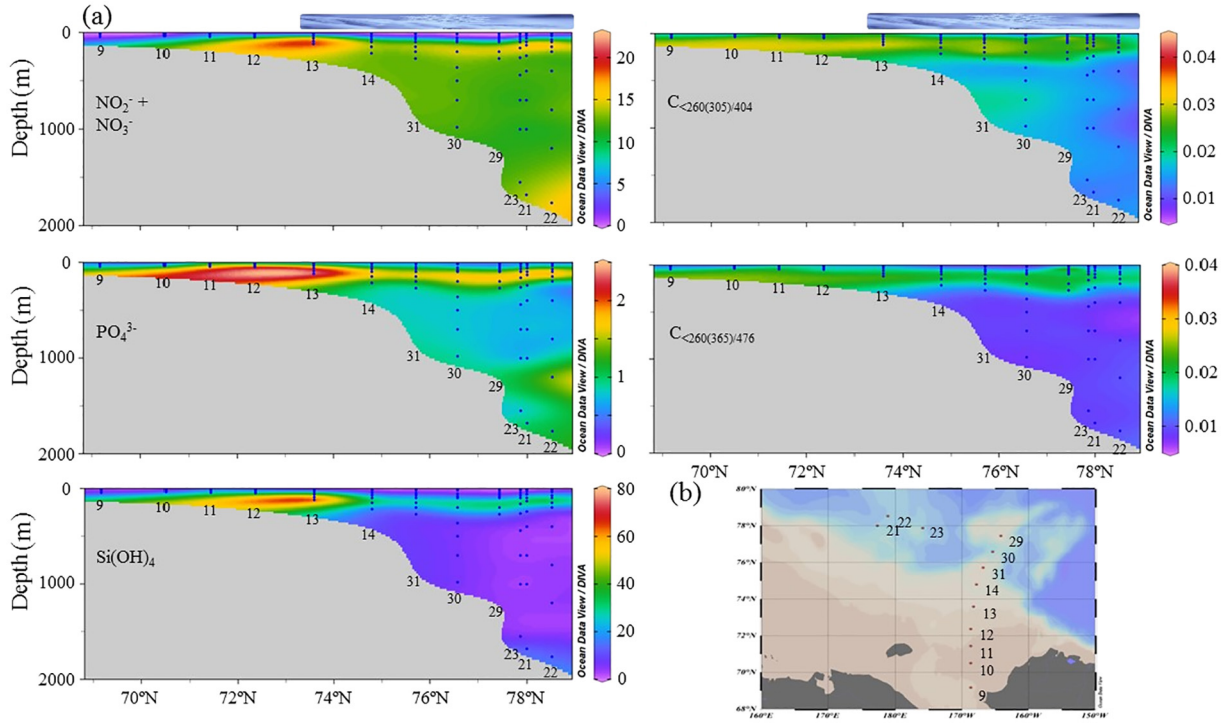

Fig. 7. Off-shelf spreading (at depth of ~100–200 m) of nutrients and humic-like FDOM in the Chukchi Sea of the Arctic Ocean (a). (b) shows the station distribution in the map. The units for nutrients and FDOM are μM and RU, respectively. The blue bars above the figures represent the sea ice cover. The numbers indicate the stations.

DOC at ice-free versus ice-covered sites suggest that the primary productivity and DOC enhancement could potentially be accelerated by sea ice retreat. In contrast, CDOM and FDOM seem to be rather insusceptible to the change of ice-cover as shown by no significant differences between the ice-free and the ice-covered sites. The reason may be associated with the primary sources of DOM in the studied regions from primary productivity in the surface ocean rather than from CDOM and FDOM-enriched terrestrial origins. The sources of the LMW DOM in surface ocean are potentially associated with inputs from the ice algae dominated by *Phaeocystis pouchetii* since the LMW fraction peak is higher for ice-covered sites than the ice-free sites where usually diatom dominates. As such, the smaller sized DOM accumulated in surface Chukchi Sea presumably is more likely to be the result from fresh primary production rather than from intense biological decomposition, which warrants further investigation.

Associated content

Notes: The authors declare no competing financial interest.

Acknowledgements

This work was supported by a National Research Foundation of Korea (NRF) grant funded by the Korea government (MSIP) (No. 2017R1A4A1015393), and the project titled 'Korea-Arctic Ocean Observing System (KOPRI, PM17040)' funded by the Ministry of Oceans and Fisheries, Korea. The authors thank the captain and crews of R/V *Araon* for help with sampling during the Arctic expedition. Special thanks also go to Dr. Boris Peter Koch for his help with the FT-ICR-MS data re-calibration and insightful comments.

Appendix A. Supplementary data

Supplementary data to this article can be found online at https://doi.org/10.1016/j.scitotenv.2018.05.205.

References

Ardyna, M., Babin, M., Gosselin, M., Devred, E., Rainville, L., Tremblay, J.-É., 2014. Recent Arctic Ocean sea ice loss triggers novel fall phytoplankton blooms. Geophys. Res. Lett. 41 (17), 6207–6212.

Assmy, P., Fernández-Méndez, M., Duarte, P., Meyer, A., Randelhoff, A., Mundy, C.J., Olsen, L.M., Kauko, H.M., Bailey, A., Chierici, M., Cohen, L., Doulgeris, A.P., Ehn, J.K., Fransson, A., Gerland, S., Hop, H., Hudson, S.R., Hughes, N., Itkin, P., Johnsen, G., King, J.A., Koch, B.P., Koenig, Z., Kwasniewski, S., Laney, S.R., Nicolaus, M., Pavlov, A.K., Polashenski, C.M., Provost, C., Rösel, A., Sandbu, M., Spreen, G., Smedsrud, L.H., Sundfjord, A., Taskjelle, T., Tatarek, A., Wiktor, J., Wagner, P.M., Wold, A., Steen, H., Granskog, M.A., 2017. Leads in Arctic pack ice enable early phytoplankton blooms below snow-covered sea ice. Sci. Rep. 7, 40850.

Bates, N.R., Cai, W.-J., Mathis, J.T., 2011. The ocean carbon cycle in the western Arctic Ocean: distributions and air-sea fluxes of carbon dioxide. Oceanography 24 (3), 186–201.

Blough, N.V., Del Vecchio, R., 2002. Chromophoric DOM in the coastal environment. In: Hansell, D.A., Carlson, C. (Eds.), Biogeochemistry of Marine Dissolved Organic Matter, 1st ed. Academic Press, New York, p. 513.

Burdige, D.J., Komada, T., Hansell, D.A., Carlson, C.A., 2015. Sediment pore waters. Biogeochemistry of Marine Dissolved Organic Matter, 2nd ed. Academic Press, Boston, Massachusetts, pp. 535–577 (p 536).

Chen, M.L., Price, R.M., Yamashita, Y., Jaffe, R., 2010. Comparative study of dissolved organic matter from groundwater and surface water in the Florida coastal Everglades using multi-dimensional spectrofluorometry combined with multivariate statistics. Appl. Geochem. 25 (6), 872–880.

Chen, M., Kim, J.-H., Nam, S.-I., Niessen, F., Hong, W.-L., Kang, M.-H., Hur, J., 2016a. Production of fluorescent dissolved organic matter in Arctic Ocean sediments. Sci. Rep. 6, 39213.

Chen, M., He, W., Choi, I., Hur, J., 2016b. Tracking the monthly changes of dissolved organic matter composition in a newly constructed reservoir and its tributaries during the initial impounding period. Environ. Sci. Pollut. Res. 23 (2), 1274–1283.

Chen, M., Kim, S., Park, J.-E., Kim, H., Hur, J., 2016c. Effects of dissolved organic matter (DOM) sources and nature of solid extraction sorbent on recoverable DOM composition: implication into potential lability of different compound groups. Anal. Bioanal. Chem. 408, 4809–4819.

Chen, M., Kim, S., Park, J.-E., Jung, H.-J., Hur, J., 2016d. Structural and compositional changes of dissolved organic matter upon solid-phase extraction tracked by multiple analytical tools. Anal. Bioanal. Chem. 408 (23), 6249–6258.

Chen, M., Nam, S.-I., Kim, J.-H., Kwon, Y.-J., Hong, S., Jung, J., Shin, K.-H., Hur, J., 2017a. High abundance of protein-like fluorescence in the Amerasian Basin of Arctic Ocean: potential implication of a fall phytoplankton bloom. Sci. Total Environ. 599–600, 355–363.

Chen, M., Kim, S.-H., Jung, H.-J., Hyun, J.-H., Choi, J.H., Lee, H.-J., Huh, I.-A., Hur, J., 2017b. Dynamics of dissolved organic matter in riverine sediments affected by weir impoundments: production, benthic flux, and environmental implications. Water Res. 121, 150–161.

Cory, R.M., McKnight, D.M., 2005. Fluorescence spectroscopy reveals ubiquitous presence of oxidized and reduced Quinones in dissolved organic matter. Environ. Sci. Technol. 39 (21), 8142–8149.

Dittmar, T., Kattner, G., 2003. The biogeochemistry of the river and shelf ecosystem of the Arctic Ocean: a review. Mar. Chem. 83 (3–4), 103–120.

Dittmar, T., Koch, B.P., Hertkorn, N., Kattner, G., 2008. A simple and efficient method for the solid-phase extraction of dissolved organic matter (SPE-DOM) from seawater. Limnol. Oceanogr. Methods 6, 230–235.

Gordon, L.I., Jennings, J.C.J., Ross, A.A., Krest, J.M., 1993. A Suggested Protocol for Continuous Flow Automated Analysis of Seawater Nutrients (Phosphate, Nitrate, Nitrite and Silicic Acid) in the WOCE Hydrographic Program and the Joint Global Ocean Fluxes Study, Oregon State University, College of Oceanic and Atmospheric Sciences, Corvallis.

Guéguen, C., McLaughlin, F.A., Carmack, E.C., Itoh, M., Narita, H., Nishino, S., 2012. The nature of colored dissolved organic matter in the southern Canada Basin and East Siberian Sea. Deep-Sea Res. II 81–84, 102–113.

Guéguen, C., Cuss, C.W., Cassels, C.J., Carmack, E.C., 2014. Absorption and fluorescence of dissolved organic matter in the waters of the Canadian Arctic archipelago, Baffin Bay, and the Labrador Sea. J. Geophys. Res. Oceans 119 (3), 2034–2047.

Guéguen, C., Itoh, M., Kikuchi, T., Eert, J., Williams, W.J., 2015. Variability in dissolved organic matter optical properties in surface waters in the Amerasian Basin. Front. Mar. Sci. 2.

Hioki, N., Kuma, K., Morita, Y., Sasayama, R., Ooki, A., Kondo, Y., Obata, H., Nishioka, J., Yamashita, Y., Nishino, S., Kikuchi, T., Aoyama, M., 2014. Laterally spreading iron, humic-like dissolved organic matter and nutrients in cold, dense subsurface water of the Arctic Ocean. Sci. Rep. 4, 6775.

Huber, S.A., Balz, A., Abert, M., Pronk, W., 2011. Characterisation of aquatic humic and non-humic matter with size-exclusion chromatography – organic carbon detection – organic nitrogen detection (LC-OCD-OND). Water Res. 45 (2), 879–885.

Huguet, A., Vacher, L., Relexans, S., Saubusse, S., Froidefond, J.M., Parlanti, E., 2009. Properties of fluorescent dissolved organic matter in the Gironde Estuary. Org. Geochem. 40 (6), 706–719.

Koch, B.P., Dittmar, T., 2006. From mass to structure: an aromaticity index for high-resolution mass data of natural organic matter. Rapid Commun. Mass Spectrom. 20, 926–932.

Lawaetz, A.J., Stedmon, C.A., 2009. Fluorescence intensity calibration using the Raman scatter peak of water. Appl. Spectrosc. 63 (8), 936–940.

Logvinova, C.L., Frey, K.E., Mann, P.J., Stubbins, A., Spencer, R.G.M., 2015. Assessing the potential impacts of declining Arctic Sea ice cover on the photochemical degradation of dissolved organic matter in the Chukchi and Beaufort seas. J. Geophys. Res. Biogeosci. 120 (11), 2326–2344.

McKnight, D.M., Boyer, E.W., Westerhoff, P.K., Doran, P.T., Kulbe, T., Andersen, D.T., 2001. Spectrofluorometric characterization of dissolved organic matter for indication of precursor organic material and aromaticity. Limnol. Oceanogr. 46 (1), 38–48.

Mendoza, W.G., Weiss, E.L., Schieber, B., Mitchell, G.B., 2017. Controls on the distribution of fluorescent dissolved organic matter during an under-ice algal bloom in the western Arctic Ocean. Glob. Biogeochem. Cycles 31 (7), 1118–1140.

Mundy, C.J., Gosselin, M., Ehn, J., Gratton, Y., Rossnagel, A., Barber, D.G., Martin, J., Tremblay, J.É., Palmer, M., Arrigo, K.R., Darnis, G., Fortier, L., Else, B., Papakyriakou, T., 2009. Contribution of under-ice primary production to an ice-edge upwelling phytoplankton bloom in the Canadian Beaufort Sea. Geophys. Res. Lett. 36 (17), L17601.

Musilova, M., Tranter, M., Wadham, J., Telling, J., Tedstone, A., Anesio, A.M., 2017. Microbially driven export of labile organic carbon from the Greenland ice sheet. Nat. Geosci. 10 (5), 360–365.

Parsons, T.R., Maita, Y., Lalli, C.M., 1984. A Manual of Chemical and Biological Methods for Seawater Analysis. Pergamon Press, Oxford.

Perrette, M., Yool, A., Quartly, G.D., Popova, E.E., 2011. Near-ubiquity of ice-edge blooms in the Arctic. Biogeosciences 8 (2), 515–524.

Rachold, V., Eicken, H., Gordeev, V.V., Grigoriev, M.N., Hubberten, H.-W., Lisitzin, A.P., Shevchenko, V.P., Schirrmeister, L., 2004. Modern Terrigenous Organic Carbon Input to the Arctic Ocean. In: Stein, R., MacDonald, R.W. (Eds.), The Organic Carbon Cycle in the Arctic Ocean. Springer Berlin Heidelberg, Berlin, Heidelberg, pp. 33–55.

Romera-Castillo, C., Sarmento, H., Alvarez-Salgado, X.A., Gasol, J.M., Marrase, C., 2010. Production of chromophoric dissolved organic matter by marine phytoplankton. Limnol. Oceanogr. 55 (1), 446–454.

Rossel, P.E., Bienhold, C., Boetius, A., Dittmar, T., 2016. Dissolved organic matter in pore water of Arctic Ocean sediments: environmental influence on molecular composition. Org. Geochem. 97, 41–52.

Sakshaug, E., 2004. Primary and secondary production in the Arctic Seas. In: Stein, R., Macdonald, R.W. (Eds.), The Organic Carbon Cycle in the Arctic Ocean. Springer-Verlag, Heidelberg, pp. 57–82.

Schlitzer, R., 2017. Ocean data view, version 4.7.10. http://odv.awi.de.

Stedmon, C.A., Bro, R., 2008. Characterizing dissolved organic matter fluorescence with parallel factor analysis: a tutorial. Limnol. Oceanogr. Methods 6, 572–579.

Stedmon, C.A., Thomas, D.N., Papadimitriou, S., Granskog, M.A., Dieckmann, G.S., 2011. Using fluorescence to characterize dissolved organic matter in Antarctic sea ice brines. J. Geophys. Res. Biogeosci. 116 (G03027).

Stein, R., 2008. Arctic Ocean sediments: processes, proxies, and paleoenvironment. In: Chamley, H. (Ed.), Developments in Marine Geology. Vol. 2. Elsevier, Oxford, UK.

Tanaka, K., Takesue, N., Nishioka, J., Kondo, Y., Ooki, A., Kuma, K., Hirawake, T., Yamashita, Y., 2016. The conservative behavior of dissolved organic carbon in surface waters of the southern Chukchi Sea, Arctic Ocean, during early summer. Sci. Rep. 6, 34123.

Uchimiya, M., Motegi, C., Nishino, S., Kawaguchi, Y., Inoue, J., Ogawa, H., Nagata, T., 2016. Coupled response of bacterial production to a wind-induced fall phytoplankton bloom and sediment resuspension in the Chukchi Sea Shelf, Western Arctic Ocean. Front. Mar. Sci. 3 (231).

Walker, S.A., Amon, R.M.W., Stedmon, C., Duan, S.W., Louchouarn, P., 2009. The use of PARAFAC modeling to trace terrestrial dissolved organic matter and fingerprint water masses in coastal Canadian Arctic surface waters. J. Geophys. Res. Biogeosci. 114 (G00F06).

Yun, M.S., Whitledge, T.E., Stockwell, D., Son, S.H., Lee, J.H., Park, J.W., Lee, D.B., Park, J., Lee, S.H., 2016. Primary production in the Chukchi Sea with potential effects of freshwater content. Biogeosciences 13 (3), 737–749.